Nanoparticle surface energy transfer (NSET) in ferroelectric liquid crystal–metallic-silver nanoparticle composites: Effect of dopant concentration on NSET parameters

T. Vimal,[1] G. H. Pujar,[2,3] K Agrahari,[1] Sanjeev R. Inamdar,[3] and R. Manohar[1,*]

[1]*Liquid Crystal Research Lab, Physics Department, University of Lucknow, Lucknow 226007, India*

[2]*Department of Physics, GM Institute of Technology, Davangere 577 006, Karnataka, India*

[3]*Laser Spectroscopy Programme, Department of Physics and UGC-CPEPA, Karnatak University, Dharwad 580003, India*

(Received 5 October 2020; accepted 28 January 2021; published 25 February 2021)

In the recent past, the resonance energy transfer studies using metallic nanoparticles has become a matter of quintessence in modern technology, which considerably extends its applications in probing specific biological and chemical processes. In the present study, metallic-silver nanoparticles of 2–4 nm (diameter) capped with hexanethiol ligand are developed and dispersed in ferroelectric liquid crystal (FLC). The morphology of nanoparticles was characterized using HR-TEM and SEM techniques. Furthermore, a systematic study of energy transfer between the host FLC material (as donors) and metallic-silver nanoparticles (as acceptors) has been explored employing steady state and time resolved fluorescence spectroscopic techniques. The nanoparticle based surface energy transfer (NSET) parameters viz., transfer efficiency, transfer rate, and proximity distance between donor and acceptor, have been determined for NSET couples (FLC material–metallic-silver nanoparticle) composites. It is observed that various NSET parameters and quenching efficiency follow a linear dependence on the concentration of metallic-silver nanoparticles in host FLC material. The nonradiative energy transfer and superquenching effect were analyzed with the help of Stern-Volmer plots. The impact of present study about superquenching effect of the silver nanoparticles can be used for sensing applications that require high degree sensitivity.

DOI: 10.1103/PhysRevE.103.022708

I. INTRODUCTION

Over the past decade nanoscience has gained prominence and the ever increasing growth has been contemplated in its advances in the field of nanomedicine, drug delivery, bioimaging, sensing, nanofabrication, etc. [1]. Among all the nanostructures, metallic nanoparticles are of interest in both research and technology, due to their specific properties not available in isolated molecules or bulk metals. Because of these properties nanoparticles have many important applications in catalysis, sensing, and imaging [2–5]. The localized surface plasmon resonance makes the metallic nanoparticles good scatterers and absorber of visible light [6]. Due to the surface characteristics and high stability of the metallic nanoparticles, they have been extensively employed as fluorescence quenchers. Highly efficient fluorescence quenching of the fluorescence of dyes and polymers (conjugated and nonconjugated) in the presence of metallic nanoparticles has been reported by several groups [7,8]. The dynamic quenching has been well explained by the process of Förster resonance energy transfer (FRET) between the FRET pairs (donor and acceptor). The energy transfer efficiency highly depends upon the relative distance between the FRET pair. In the case of metallic nanoparticles, energy transfer between the donor-acceptor pair can be termed as nanoparticle based surface energy transfer (NSET) due to the dipole-surface type energy transfer [9]. The efficiency of NSET is usually high over FRET. Fluorescence lifetime is a more reliable parameter to validate the possibility of energy transfer in a system, as it is largely independent of the fluorescence intensity and fluorophore concentration. Time resolved fluorescence measurements also provide significant and precise information about the molecular interactions in comparison to the steady state measurements [10].

The chemically tailored tunable optoelectronic properties, shapes, and size of metallic nanoparticles such as gold, silver, copper, etc. make them suitable to be used as dopant in liquid crystals (LCs). The incorporation of metallic nanoparticles could effectively improve the optical, electrical, and dielectric properties of the LC material [11–14]. Dispersion of a small quantity of metallic nanoparticles can efficiently influence the fluorescence properties of host liquid crystalline material [15–17]. However, in literature, changes in fluorescence intensity of host FLC material in the presences of metallic nanoparticles has not been discussed by considering FRET or NSET mechanism.

In the present article we have investigated the interaction of hexanethiol capped silver nanoparticles with ferroelectric liquid crystalline material. Absorbance and florescence properties of the FLC material in the presence of silver nanoparticles have been studied. Steady-state measurements reveal the fluorescence quenching of FLC material after the dispersion of metallic-silver nanoparticles. Time-resolved fluorescence spectroscopic techniques have been used to confirm the results obtained from the steady-state measurements.

*Corresponding author: rajiv.manohar@gmail.com

In order to ascertain the type of energy transfer occurring between the FLC host material and silver nanoparticles (donor-acceptor pair), results obtained from the above mentioned techniques have been further analyzed. The possibility of FRET and NSET mechanism between the donor-acceptor pair has been checked and discussed. The superquenching effect is analyzed using Stern-Volmer plots. The NSET parameters, i.e., efficiency of energy transfer and transfer rate, are found to be linearly dependent on the concentration of metallic-silver nanoparticles in host FLC material. The present investigation may deepen our understanding of the photophysical properties of mesogenic FLC material–silver-nanoparticles pair and their possible applications in biological and chemical processes and exploitation of silver nanoparticles in biosensing applications.

II. MATERIALS AND METHODS

FLC material W343 has been used as host material. It differs from other types of ferroelectric materials as they have only fluorinated terphenyl compounds in composition [18–20].

In the present work the metallic-silver nanoparticles (AgNPs) of 2–4 nm (diameter) capped with hexanethiol ligand are used as dopant. The morphology of nanoparticles was characterized using HR-TEM and SEM. The HR-TEM images confirm the homogeneous size distribution of silver nanoparticles [21].

The silver nanoparticles have been dispersed in host FLC in 0.1, 0.3, and 0.5 (wt./wt.)% concentration. The pure FLC material is termed as $\mathbf{S_0}$, whereas composite samples are written as $\mathbf{S_1}$ [FLC W343+0.1(wt./wt.)% AgNPs], $\mathbf{S_2}$ [FLC W343+0.3(wt./wt.)% AgNPs], and $\mathbf{S_3}$ [FLC W343+ 0.5(wt./wt.)% AgNPs] in the entire article. Detailed procedure of composite preparation has already been described in our paper [22].

The optical measurements were done in toluene solutions at room temperature. The UV-visible absorption spectra were recorded using a UV-Vis-NIR spectrophotometer (JASCO, model V-670). Fluorescence emission spectra were obtained from a spectrofluorometer (JY Horiba, Floromax-4). A specially designed quartz cell of 10 mm optical path length was used for all the spectra. Fluorescence quantum yields (Φ) of pure FLC material were estimated by comparing wavelength-integrated photoluminescence intensity of the pure FLC material with that of the reference, following standard procedure [23].

The interaction of the silver nanoparticles with FLC material can be studied by monitoring their effect on the exciton lifetime by using fluorescence lifetime measurements. The time resolved fluorescence decay profiles were collected by using a time domain spectrometer (ISS, ChronosBH) based on the time-correlated single photon counting (TCSPC) technique. All the samples were excited at 275 nm using a Horiba make laser diode as excitation source having instrument response function ~560 ps and peak power ~45 mW. The signals were collected at the magic angle of 57.5° to eliminate the contribution from anisotropy decay. The time-resolved decays were collected by PMT (Hamamatsu, model H5773), a fast detector. The decay profiles were analyzed using vinci multidimensional fluorescence spectroscopy software. The time-resolved decays are fitted with tri-exponential function $I(t) = (\tau_1 A_1 + \tau_2 A_2 + \tau_3 A_3)$ where τ_1, τ_2, and τ_3 represent the shorter, longer, and longest lifetime components with their normalized amplitude components A_1 A_2, and A_3, respectively and the average lifetime $\langle\tau\rangle$ was calculated using the following equation:

$$\langle\tau\rangle = \frac{(\tau_1 A_1 + \tau_2 A_2 + \tau_3 A_3)}{A_1 + A_2 + A_3}. \quad (1)$$

The acceptability of the fits was judged from the $\chi 2$ criterion and the residual of the functions fitted to the actual data [24].

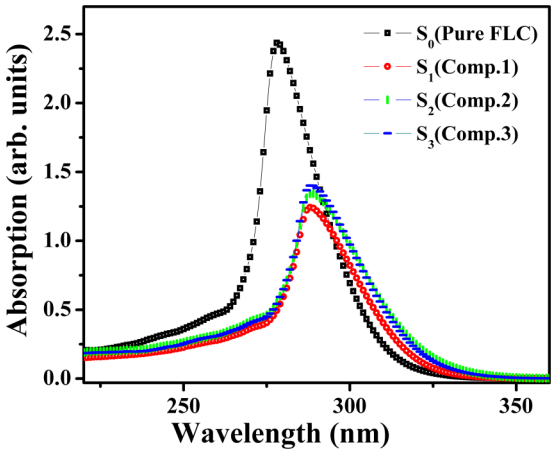

FIG. 1. UV absorbance of host FLC material ($\mathbf{S_0}$) and FLC composites having metallic-silver nanoparticles in 0.1, 0.3, and 0.5 (wt./wt.)% concentration ($\mathbf{S_1}$, $\mathbf{S_2}$, $\mathbf{S_3}$). Absorbance study has been performed in colloidal state (at room temperature) by taking HPLC grade toluene (mg/ml) as solvent.

III. RESULTS AND DISCUSSION

Absorbance is a fundamental and practically important parameter for any LC material. For electro-optical application of a liquid crystal device, light absorption in a particular region of wavelength could be a topic of interest. As the absorbed light converts into the thermal energy, it consequently changes the temperature of the LC material. The physical properties of a thermotropic LC device are temperature dependent and will be affected by the absorbance of light by the LC cell. Absorbance of light by LC material also gives the information about its photostability and electronic transitions. The major absorbance of light by an LC material occurs in two spectral regions: Ultraviolet (UV) and infrared (IR). The absorbance reflects both the size of the fluorophore and the probability that light of a given wavelength will be absorbed when it strikes the fluorophore. Liquid crystal materials have many optical applications and it is necessary to understand its light absorbing efficiency. Figure 1 shows the absorption spectra of pure FLC and silver nanoparticles dispersed FLC composites.

$\mathbf{S_0}$ (pure FLC material) shows a single absorbance peak at 278 nm. The absorption peak position (in terms of wavelength) denotes the energy associated with the quantum mechanical change in the material after the energy

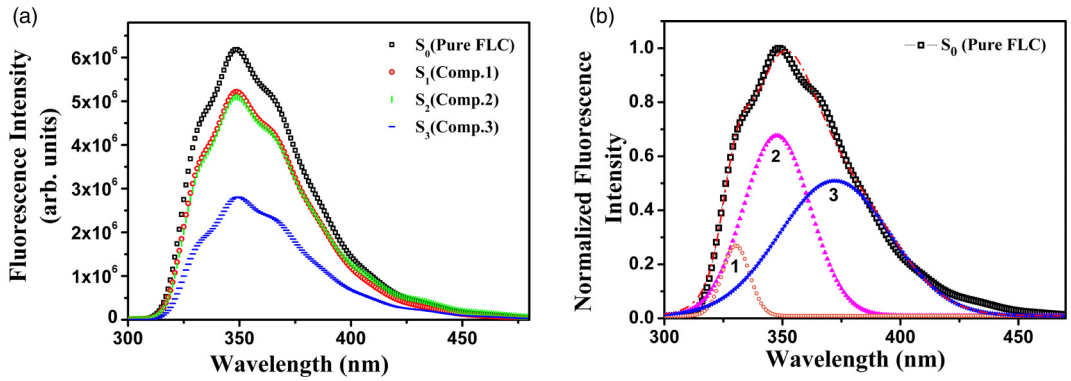

FIG. 2. (a) Fluorescence spectra of $\mathbf{S_0}$ (pure FLC material) and $\mathbf{S_1}$, $\mathbf{S_2}$, $\mathbf{S_3}$ (FLC–metallic-silver nanoparticles composites). (b) The Gaussian fit of the fluorescence spectra of $\mathbf{S_0}$ (pure FLC material).

absorption. The absorption of $\mathbf{S_0}$ is in between the 180–400 nm wavelength range of UV region and is attributed to $\pi \rightarrow \pi^*$ electronic transitions. All the composites show the characteristic absorption peak of $\mathbf{S_0}$ with no additional absorption. A shift in the peak position as well as a significant decrement in the absorbance intensity after the dispersion of nanoparticles can be seen from Fig. 1. The peak position is now centered at 288 nm which means it is shifted towards the higher wavelength region. A shift of about 10 nm in absorption maxima of $\mathbf{S_0}$ after the nanoparticles dispersion indicates that some kind of conjugation mechanism is taking place between the nanoparticles and FLC material. The longer the molecular conjugation in a material, the longer the absorption wavelength. The conjugation mechanism between the nanoparticles and FLC material will be discussed in a subsequent part of the article. An almost 50% decrease or reduction in the absorbance intensity for $\mathbf{S_1}$ has been observed. The intensity and wavelength of an electronic transition band determines the refractive index and birefringence of an LC material. Such an enormous change in absorbance intensity can be attributed to the change in the refractive index of the medium (FLC material) after the dispersion of NPs [25]. A slight intensification in the absorbance intensity can be seen further with the increase of NPs concentration in FLC (for $\mathbf{S_2}$ and $\mathbf{S_3}$). Silver nanoparticles are extraordinarily efficient at absorbing and scattering light. The strong interaction of light with silver nanoparticles occurs because the conduction electrons on the metal surface undergo a collective oscillation known as surface plasmon resonance (SPR), these collective oscillation results in unusually strong scattering and absorption properties of the silver nanoparticles [26,27]. The small increment in UV absorbance intensity for $\mathbf{S_2}$ and $\mathbf{S_3}$ might be due to the strong absorption property of the NPs. However, it is still lower than that of $\mathbf{S_0}$ (pure FLC material) as the concentration of NPs is very small in the composites.

Figure 2(a) shows the fluorescence spectra of pure FLC and composites having varying wt./wt.% concentration of nanoparticles. 278 nm is the excitation wavelength for all the samples under consideration. The primary fluorescence emission of $\mathbf{S_0}$ is centered at 350 nm. As can be seen from Fig. 2(a) the emission spectrum of $\mathbf{S_0}$ is broad in nature and it consists of two or more submerged components. With the help of Gaussian fit, its three submerged components have been obtained and presented in Fig. 2(b). The three submerged components of PL peak of $\mathbf{S_0}$ obtained from the Gaussian fit were found to be centered at 330, 347, and 372 nm. The shape of emission peak for three composites ($\mathbf{S_1}$, $\mathbf{S_2}$, $\mathbf{S_3}$) hardly changes, which means that after the dispersion of nanoparticles the emission peak shape is still broad in nature. The position of emission peaks also remained unaltered for composites. So it can be concluded that in the NPs dispersed LC systems, apart from the decrease in the emission intensity, shape, and position of the emission peak remains unchanged. This indicates that nanoparticles are participating in the energy transfer process rather than affecting the emission properties of host FLC material.

It is clear from Fig. 2(a) that the dispersion of NPs causes a significant quenching of fluorescence intensity of $\mathbf{S_0}$ (pure FLC material). Various research groups [28,29] have already reported the quenching of fluorescence intensity of the LC system in the presence of silver-metallic nanoparticles. The observed quenching of emission intensity of $\mathbf{S_0}$ is about 44% when combined with maximum concentration of silver nanoparticles [0.5 (wt./wt.)% AgNPs] used in the present study. Significant quenching indicates that a kind of energy transfer mechanism is taking place in the composite system. As suggested by Gersten–Nitzan (GN) theory, the metallic nanoparticles have a strong electric field and when a dipolar entity is placed close to a metallic nanoparticle there will be changes in the radiative and nonradiative rates of decay due to coupling of the dipolar entity to the metal's local electric field [30]. As the fluorescence intensity is proportional to the rate of radiative recombination, quenching of emission intensity envisages that the metallic nanoparticles are responsible for altering the radiative rate of fluorophore $\mathbf{S_0}$ (pure FLC material). The radiative decay rate constant (or fluorescence rate constant) of a fluorophore presents a fundamental photophysical property. For better understanding of quenching process, the radiative decay rates are calculated by using the following equation:

$$k_r = 3.13 \times 10^{-9} \nu_0^2 \int \varepsilon d\bar{\nu} \cong \nu_0^2 f. \tag{2}$$

Here ν_0 is the energy in wave numbers obtained from the absorption maximum of the $\mathbf{S_0}$, f is the oscillator strength (strength of the pertinent electronic transition), and ε is the

TABLE I. Various parameters calculated using the NSET theory for FLC material and nanoparticles energy transfer pair with the varying concentration of NPs in FLC.

System	d_0(Å)	d(Å)	ϕ_{ET}(%)	$k_{SET}(S^{-1})$	$k_r(S^{-1})$
S_0 (pure FLC)					22.1×10^7
S_1 (composite 1)	116	222	6.97	3.29×10^8	17.1×10^7
S_2 (composite 2)	116	175	16.14	8.44×10^8	16.7×10^7
S_3 (composite 3)	116	146	28.38	17.4×10^8	11.9×10^7

molar extinction coefficient. An almost 54% decrement in the oscillator strength has been obtained for $\mathbf{S_3}$. That is very considerably comparable to the PL intensity quenching (about 50%) for $\mathbf{S_3}$.The calculated radiative decay rates [$k_r(S^{-1})$] for $\mathbf{S_0}$ and $\mathbf{S_3}$, are 2.21×10^8 and 1.19×10^8 S^{-1} (as mentioned in Table I), respectively. Here it can be inferred that the PL quenching of FLC material after the dispersion of silver nanoparticles is definitely due to energy transfer between the two via some energy transfer mechanism.

The energy transfer manifests itself through the quenching of donor fluorescence and a decrease in the value of excited state lifetime accompanied by an increase in acceptor fluorescence intensity. The energy transfer between the donor and acceptor pair is usually explained by the FRET mechanism [31]. The prerequisite for energy transfer is that the emission spectrum of the donor entity must overlap adequately with the absorption spectrum of the acceptor entity.

Figure 3 shows the absorption spectra of silver nanoparticles and emission spectra of $\mathbf{S_0}$. In the absorption spectra of silver nanoparticles, a strong absorption peak at 292 nm and other small absorption peaks at lower wavelength regions can be observed. These small peaks might be due to plasmon bands for silver nanoparticles. Figure 3 also shows the spectral overlap between fluorescence emission spectra of $\mathbf{S_0}$ (pure FLC) and absorption spectra of silver nanoparticles. It can be seen that the absorption bands of silver nanoparticles overlap with emission bands of $\mathbf{S_0}$ around 350 nm. Overlap integral between the emission spectra of $\mathbf{S_0}$ and silver nanoparticles is

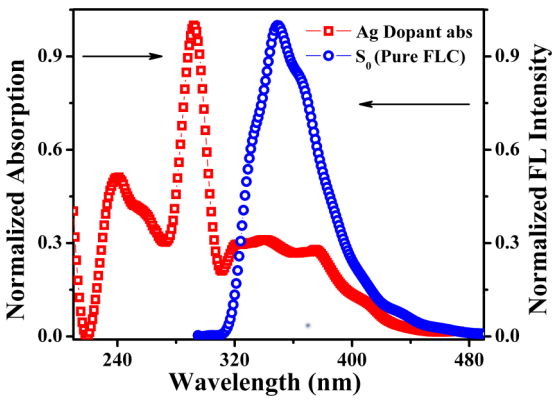

FIG. 3. Spectral overlap between fluorescence spectra of pure FLC (blue circle) and absorption spectra of metallic-silver nanoparticles [Ag dopant (red square)], at room temperature.

being calculated by the following equation:

$$J(\lambda) = \int_0^\infty F_D(\lambda)\varepsilon_A(\lambda)\lambda^4 d\lambda. \tag{3}$$

The overlap integral mainly depends upon the $F_D(\lambda)$, the corrected florescence intensity of the donor in the wavelength range λ to $\lambda + \Delta\lambda$, with the integral intensity (area under the curve) normalized to unity and $\varepsilon_A(\lambda)$, the extinction coefficient of the acceptor at λ, in units of $M^{-1}\,cm^{-1}$. The value of overlap integral between the emission spectra of $\mathbf{S_0}$ and silver nanoparticles calculated from the above equation has come out to be $8.11 \times 10^{-15}\,M^{-1}\,cm^3$. Partial overlap of surface plasmon resonance band of silver nanoparticles with the emission band of pure FLC endorses the occurrence of energy transfer between $\mathbf{S_0}$ (pure FLC material) and silver nanoparticles. In the present composite system [FLC material ($\mathbf{S_0}$) and silver NPs (AgNPs)], the nanoparticles are functioning as energy acceptors and the mesogenic FLC material as an energy donor.

Initially we have considered the theoretical model of FRET (Förster resonance energy transfer) to explain the quenching of the emission intensity of $\mathbf{S_0}$ in the presence of silver nanoparticles. The FRET mechanism involves the radiationless transfer of energy from donor fluorophore to an acceptor fluorophore. This mechanism results from dipole-dipole interaction and strongly depends on the center to center distance of donor and acceptor. According to the FRET theory [31], the rate of energy transfer for donor acceptor pair separated by distance r is given by

$$k_T(r) = \frac{1}{\tau_d}\left(\frac{R_0}{r}\right)^6. \tag{4}$$

Here τ_d is lifetime of donor in the absence of acceptor and r is the donor-acceptor distance. R_0 is the Förster distance and defined as the distance at which half of the energy is transferred to the acceptor. It depends upon the spectral properties of the donor and acceptor. It can be written in the mathematical form as

$$R_0 = 0.211[k^2 n^{-4}\varphi_d J(\lambda)]^{1/6}. \tag{5}$$

Here k^2 is the orientation factor, ϕ_d is the quantum efficiency of donor in the absence of acceptor, $J(\lambda)$ is the spectral overlap integral between the acceptor absorption and donor emission, and n is the refractive index of the medium. A relative optical method has been used to determine the fluorescence quantum yield of the $\mathbf{S_0}$ (host FLC material) [23].

For the composite system $\mathbf{S_3}$, computed radiative transfer rate is found to be $2.31 \times 10^8\,S^{-1}$. The calculated Förster distance (R) and the calculated proximity donor-acceptor distance (r) for $\mathbf{S_3}$ by FRET model are found to be 263 and 136 Å, respectively. Since it is well known from the literature and reports about the energy transfer between the energy transfer pair (ETP), FRET has a limited operational range of 10–80 Å distance between donor and acceptor [32]. It is restricted by the upper limit of ~80 Å. Hence, for the present energy transfer pair (host FLC material and silver nanoparticles), the FRET model cannot be utilized. Limitation of the FRET has led us to explore the long range plasmonic nanoparticles surface energy transfer (NSET) model to study

the energy transfer between the host FLC material and silver nanoparticles. It has been suggested by Yun *et al.* that the FRET barrier can be overcome through nanoparticles based surface energy transfer (NSET) for the metallic nanoparticles and fluorophore systems [33]. In the past few years the NSET model has become a matter of interest as this is capable of measuring distances nearly twice as far as FRET. This model aids us to understand the conformational dynamics of compound biomolecules in macroscopic detail.

In the nanoparticles surface energy transfer (NSET) model, when a metallic nanoparticle and a dipolar entity are brought into close proximity, they undergo dipole surface type energy transfer from the dipolar donor entity to the metallic nanoparticle surface. Here it can be assumed that the nanoparticle is a molecule and the surfaces of the nanoparticles are not causing any perturbation in dipolar entity [34]. The presence of nanoparticles modifies the excited state deactivation corridors of the fluorophore. The surface energy transfer is highly dependent on the interaction of the electromagnetic field of the donor dipole with the conduction band's delocalized electrons of metallic nanoparticles. These delocalized electrons provide dipole vectors on the surface of the nanoparticle to make it ready to accept energy from the donor. Thus they behave as the energy acceptor. These delocalized conduction electrons interact very strongly with the oscillating dipole of the fluorophore when they are in close proximity and perpendicular. The efficiency of NSET process depends on the inverse fourth power (d^{-4}) of the donor-acceptor distance [35]. The rate of energy transfer from dipole-surface interaction can be written in mathematical form as

$$k_{\mathrm{SET}} = \frac{1}{\tau_d}\left(\frac{d_0}{d}\right)^4. \tag{6}$$

Here d is the donor-acceptor distance and d_0 is the distance at which a donor entity has equal probabilities for energy transfer and spontaneous emission. d_0 can be calculated using Persson model [36,37]:

$$d_0 = \left(\frac{0.225c^2\phi_{\mathrm{donor}}}{\omega^2_{\mathrm{donor}}\omega_F k_F}\right)^{1/4}. \tag{7}$$

Here Φ_{donor} is the quantum efficiency of donor entity, the frequency of the donor electronic transition (ω_{donor}), the Fermi frequency (ω_F), and Fermi wave vector (k_F) of the metallic nanoparticles [9]. Accordingly, the value of d_0 has been calculated using $\Phi_{\mathrm{donor}} = 0.35$, $\omega_{\mathrm{d}} = 4.67 \times 10^{15}\ \mathrm{s}^{-1}$, $\omega_{\mathrm{F}} = 8.4 \times 10^{15}\ \mathrm{s}^{-1}$, $k_F = 1.2 \times 10^8\ \mathrm{cm}^{-1}$, and $c = 3 \times 10^{10}\ \mathrm{cm\,s}^{-1}$.

The donor-acceptor distance (d) is calculated using the following equation:

$$\phi_{\mathrm{ET}} = \frac{1}{1 + \left(\frac{d}{d_0}\right)^4}. \tag{8}$$

Here ϕ_{ET} is energy transfer efficiency in the NSET process, which can be estimated using steady state and time resolved data according to the equation $\Phi_{\mathrm{ET}} = 1 - (F_{da}/F_d) = 1 - (\tau_{da}/\tau_d)$, where F_{da} and F_d are the relative fluorescence intensities of the fluorescence donor in the presence and absence of the acceptor, respectively, and τ_{da} and τ_d are the lifetimes of the donor with and without the acceptor. The various NSET parameters have been calculated and presented in Table I.

It can be observed from Table I that the values of k_{SET} (rate of energy transfer from dipole to surface) and ϕ_{ET} (energy transfer efficiency) are increasing linearly with the concentration of silver nanoparticles in host FLC material. The donor-acceptor distance (d) has also been found to decrease with the increasing concentration of nanoparticles in the host FLC material. The interaction between the fluorophore (FLC material) and metallic nanoparticle is strongly dependent on the distance between them. A short distance will lead to strong interaction and a subsequent high k_{SET} value for composite systems. It is worth noting that the transfer efficiency value increases as the intermolecular distance decreases. It confirms distance dependent energy transfer efficiency in the present NSET couple.

From the above calculated parameters (Table I) it can be inferred that an efficient nonradiative resonance energy transfer is taking place from the dipolar mesogenic molecules to the metallic-silver nanoparticles. Due to the close proximity of the two, the molecular dipole of the mesogenic molecule is damped by the nearby metallic surface. The relative orientation of the mesogenic molecule's dipole moment with respect to the metallic nanoparticles surface governs the radiative rate of the composite system. From Table I it can be seen that the radiative rate decreases with the increasing concentration of nanoparticles in the host FLC material. It predicts that the molecular dipole of the mesogenic material is tangentially oriented towards the metallic surface and both the dipoles radiate out of phase. Therefore, the energy transfer from FLC material to metallic-silver nanoparticles is positively governed by the NSET process and it follows the $1/d^4$ distance dependent relation. The time resolved fluorescence study has also been done and discussed as follows for further confirmation of energy transfer between the dipolar mesogenic molecules and metallic-silver nanoparticles surface.

A time-resolved fluorescence lifetime measurement is an absolute measurement, unlike the steady state intensity, in which one is relative. The fluorescence lifetime is an intrinsic molecular property and within certain constraints it is independent of concentration. This means that changes in concentration caused either by photobleaching or diluting or concentrating the sample, would not affect the lifetime value. This is in contrast to a steady state measurement, where a change in concentration causes a subsequent change in the intensity of the recorded emission. Hence, it is a precise parameter to confirm the energy transfer between donor and acceptor pair [38]. Dispersion of metallic-silver nanoparticles can affect the intrinsic decay rate of the host FLC material, which can be observed by the fluorescence lifetime decay of the FLC material. The decay of the excited state of a molecule to the ground state can be expressed as

$$I(t) = I_0 \exp(-t/\tau). \tag{9}$$

Here I_0 is the intensity at zero time (upon excitation) and τ is the fluorescence lifetime. The fluorescence lifetime is defined as the time for the fluorescence intensity to drop by $1/e$ or to ~37%. The parameters of $I(t)$ are usually abstracted by the nonlinear fitting combined with deconvolution procedure.

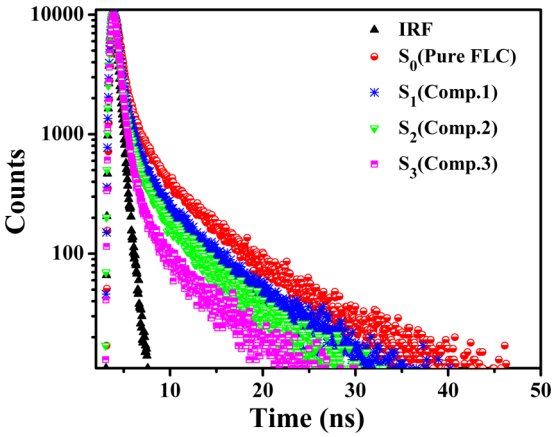

FIG. 4. Time-resolved decay profile of pure FLC material ($\mathbf{S_0}$) along with FLC–metallic-silver nanoparticles composites ($\mathbf{S_1}$, $\mathbf{S_2}$, $\mathbf{S_3}$) at room temperature.

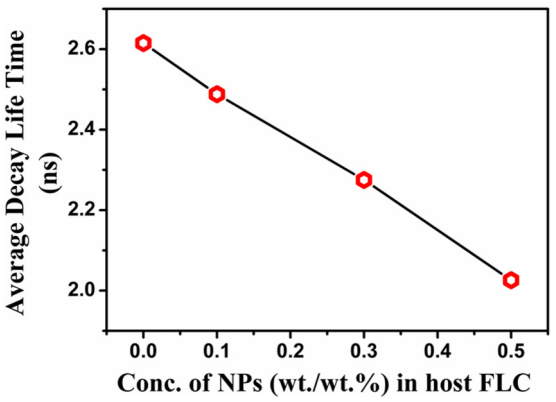

FIG. 5. Average decay lifetime of host FLC material as a function of metallic-silver nanoparticles concentration in host LC material.

In the case of multiexponential decay (at least three distinct lifetimes), the equation can be written in mathematical form:

$$I(t) = I_0 \sum A_i e^{(-t/\tau_i)}. \tag{10}$$

An analogous analysis is performed in the case of multiexponential decay to extract lifetimes (τ_i) and fractions (A_i). Figure 4 shows the decay profile of $\mathbf{S_0}$ (pure FLC) in the absence and presence of metallic nanoparticles at room temperature.

The decay profile is based on varying weight concentration of nanoparticles in $\mathbf{S_0}$. All energy transfer pairs have exhibited tri-exponential decay time (see Table II). The average decay lifetime ($\langle\tau\rangle$) has been calculated from the equation described in the experimental section. The fractions, corresponding amplitudes, and lifetime values are listed in Table II for each system. Reduction in lifetime for a donor-acceptor system is one of the characteristic features of efficient energy transfer. The average photoluminescence decay profiles for $\mathbf{S_0}$ (pure FLC) and all three composites ($\mathbf{S_1}$, $\mathbf{S_2}$, $\mathbf{S_3}$) are presented in Fig. 5. Here we can see that the lifetimes of pure FLC was shortened after the dispersion of metallic-silver nanoparticles.

The transfer efficiency was calculated using $\Phi_{\mathrm{ET}} = 1 - (\tau_{da}/\tau_d)$. The transfer efficiency increases linearly with the nanoparticles concentration in host FLC material and the same trend is observed from the steady state measurements. The fluorescence lifetime depends upon the rate constants; radiative rate (k_r), nonradiative rate (k_{nr}), and can be written as

$$\tau = \frac{1}{k_r + k_{\mathrm{nr}}}. \tag{11}$$

A reduction in lifetime of host FLC material in the presence of nanoparticles is due to the nonradiative energy transfer from FLC material to the conduction band's delocalized electrons of the metallic-silver nanoparticles. As mentioned earlier, the presence of NPs decreases the radiative decay rate of FLC material. Subsequently, a significant reduction in the excited state lifetime or fluorescence lifetime of FLC material occurs in the presence of nanoparticles. An almost linear correlation between the fluorescence lifetime and concentration of nanoparticles indicates that the higher dopant concentration means more absorbing entities in the composite system.

The observed superquenching effect in the present investigation was analyzed for time resolved measurements employing Stern-Volmer (SV) plots [23,32,39].

As $F_d/F_{da} = 1 + K_{SV}[Q] = 1 + k_q\tau_d[Q] = \tau_d/\tau_{da}$, where F_d and F_{da} are the fluorescence intensity of donor (FLC) in the absence and presence of quencher (silver NPs), K_{SV} is the quenching constant, k_q is the rate constant of the bimolecular process, $[Q]$ is the quencher concentration, while τ_d and τ_{da} are the average fluorescence lifetimes of the fluorophore FLC material without and with the silver NPs, respectively. For the three composite systems, we get three different values of the ratio τ_d/τ_{da}. These values have been plotted against the concentration of nanoparticles in FLC material and shown in Fig. 6.

From the linear plot of Fig. 6, the slope gives K_{SV} value and found to be $8.13 \times 10^9\,\mathrm{M}^{-1}$. The calculated bimolecular quenching rate constant ($k_q = K_{SV}/\tau_d$) value is $3.11 \times 10^{18}\,\mathrm{M}^{-1}\,\mathrm{s}^{-1}$. These values are much larger than diffusion controlled quenching rate constant ($k_d \sim 10^{10}\,\mathrm{M}^{-1}\,\mathrm{s}^{-1}$) [23,39,40]. Thus, in the present study quenching is not controlled by diffusion process. Furthermore, the high values of

TABLE II. Lifetime values and fractions obtained from time-resolved study of $\mathbf{S_0}$, $\mathbf{S_1}$, $\mathbf{S_2}$, and $\mathbf{S_3}$.

System	τ_1 (ns)	τ_2 (ns)	τ_3 (ns)	A_1	A_2	A_3	Average $\langle\tau\rangle$ (ns)	ϕ_{ET}(%)
Pure FLC ($\mathbf{S_0}$)	0.754	1.238	6.480	48.61	20.63	30.76	2.615	
$\mathbf{S_1}$ (composite 1)	0.713	1.478	6.473	57.25	13.76	28.99	2.488	4.85
$\mathbf{S_2}$ (composite 2)	0.742	1.263	6.314	54.39	19.95	25.66	2.275	12.98
$\mathbf{S_3}$ (composite 3)	0.716	1.276	5.889	60.93	15.42	23.66	2.026	22.52

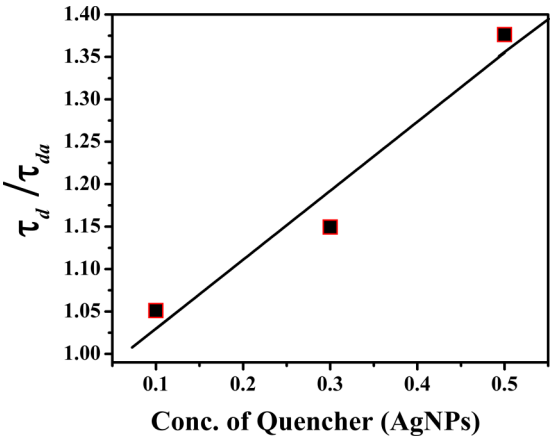

FIG. 6. The time resolved Stern-Volmer plot for NSET pair: Host FLC material–metallic-silver nanoparticles.

K_{SV} and k_q implies that superquenching is due to the efficient nonradiative energy transfer from FLC to metallic-silver nanoparticles.

In the light of the above superquenching process and calculated NSET parameters, it can be concluded that an efficient nonradiative nanoparticle surface energy transfer is taking place from FLC material to metallic-silver nanoparticles.

IV. CONCLUSIONS

In this paper we have studied the effect of dispersion of metallic-silver nanoparticles on the fluorescence and absorption properties of the host ferroelectric liquid crystalline material. The interaction between the host FLC material and metallic-silver nanoparticles has been systematically studied employing steady state and time resolved measurements. The steady state fluorescence spectrum of composite systems shows that the fluorescence from mesogenic molecules has been quenched by metallic-silver nanoparticles. Quenching of fluorescence intensity is attributed to the NSET mechanism as the distance between donor-acceptor pair is large and beyond the range predicted by Fröster resonance energy transfer. The FLC material (the donor entity) and metallic-silver nanoparticles (the acceptor entity) are the new NSET couple as observed in the present study. A significant shortening of fluorescence lifetime of FLC material after dispersion of nanoparticles validates the occurrence of nonradiative resonance energy transfer in the present NSET couple. Furthermore, super quenching effect of silver NPs was analyzed using Stern-Volmer plots which inferred that the superquenching is not a diffusion controlled mechanism. It is due to nonradiative energy transfer from FLC to silver NPs. Tailoring of fluorescence properties of FLC material in the presence of metallic nanoparticles shows its utilization in the energy transfer based real-time applications.

ACKNOWLEDGMENTS

Authors are thankful to Professor P. Ramamurthy and Dr. Selvaraju, National Centre for Ultrafast Processes, Chennai, for time-resolved measurements and also to the University Scientific Instruments Centre, Karnatak University, Dharwad for technical help.

[1] D. A. Giljohann and C. A. Mirkin, Drivers of biodiagnostic development, Nature (London) **462**, 461 (2009).
[2] N. L. Rosi and C. A. Mirkin, Nanostructures in biodiagnostics, Chem. Rev. **105**, 1547 (2005).
[3] S. Link, Z. L. Wang, and M. A. El-Sayed, Alloy formation of gold−silver nanoparticles and the dependence of the plasmon absorption on their composition, J. Phys. Chem. B **103**, 3529 (1999).
[4] G. M. Whitesides, The right size in nanobiotechnology, Nat. Biotechnol. **21**, 1161 (2003).
[5] E. Hutter and J. H. Fendler, Exploitation of localized surface plasmon resonance, Adv. Mater. **16**, 1685 (2004).
[6] P. K. Jain, K. S. Lee, I. H. El-Sayed, and M. A. El-Sayed, Calculated absorption and scattering properties of gold nanoparticles of different size, shape, and composition: Applications in biological imaging and biomedicine, J. Phys. Chem. B **110**, 7238 (2006).
[7] H. Li and L. Rothberg, Colorimetric detection of DNA sequences based on electrostatic interactions with unmodified gold nanoparticles, Proc. Natl. Acad. Sci. U.S.A. **101**, 14036 (2004).
[8] J. Zhang, Y. Fu, M. H. Chowdhury, and J. R. Lakowicz, Enhanced Förster resonance energy transfer on single metal particle. 2. Dependence on donor−acceptor separation distance, particle size, and distance from metal surface, J. Phys. Chem. C **111**, 11784 (2007).
[9] P. C. Ray, Z. Fan, R. A. Crouch, S. S. Sinha, and A. Pramanik, Nanoscopic optical rulers beyond the FRET distance limit: Fundamentals and applications, Chem. Soc. Rev. **43**, 6370 (2014).
[10] D. V. O. O'Connor, W. R. Ware, and J. C. Andre, Deconvolution of fluorescence decay curves. A critical comparison of techniques, J. Phys. Chem. **83**, 1333 (1979).
[11] S. Tripathi, P. Ganguly, D. Haranath, W. Haase, and A. M. Biradar, Optical response of ferroelectric liquid crystals doped with metal nanoparticles, Appl. Phys. Lett. **102**, 063115 (2013).
[12] S. Y. Huang, C. C. Peng, L. W. Tu, and C. T. Kuo, Enhancement of luminescence of nematic liquid crystals doped with silver nanoparticles, Mol. Crystallogr. Liq. Crystallogr. **507**, 301 (2009).
[13] S. Kaur, S. P. Singh, A. M. Biradar, A. Choudhary, and K. Sreenivas, Enhanced electro-optical properties in gold nanoparticles doped ferroelectric liquid crystals, Appl. Phys. Lett. **91**, 023120 (2007).
[14] Y. Zhang, Q. Liu, H. Mundoor, Y. Yuan, and I. I. Smalyukh, Metal nanoparticle dispersion, alignment, and assembly in nematic liquid crystals for applications in switchable plasmonic color filters and e-polarizers, ACS Nano. **9**, 3097 (2015).

[15] R. Pratibha, K. Park, I. I. Smalyukh, and W. Park, Tunable optical metamaterial based on liquid crystal-gold nanosphere composite, Opt. Express **17**, 19459 (2009).

[16] M. Middha, R. Kumar, and K. K. Raina, Photoluminescence tuning and electro-optical memory in chiral nematic liquid crystals doped with silver nanoparticles, Liq. Crystallogr. **43**, 1002 (2016).

[17] A. Kumar, J. Prakash, D. S. Mehta, A. M. Biradar, and W. Haase, Enhanced photoluminescence in gold nanoparticles doped ferroelectric liquid crystals, Appl. Phys. Lett. **95**, 02317 (2009).

[18] M. Tykarska, R. Dąbrowski, M. Czerwiński, A. Chełstowska, W. Piecek, and P. Morawiak, Pyrimidine-based ferroelectric mixtures—The influence of oligophenyl based chiral doping system, Phase Trans. **85**, 364 (2012).

[19] K. Kurp, M. Czerwiński, and M. Tykarska, Ferroelectric compounds with chiral (S)-1-methylheptyloxycarbonyl terminal chain—Their miscibility and a helical pitch, Liq. Crystallogr. **42**, 248 (2015).

[20] K. Kurp, M. Czerwiński, M. Tykarska, and A. Bubnov, Design of advanced multicomponent ferroelectric liquid crystalline mixtures with submicrometre helical pitch, Liq. Crystallogr. **44**, 748 (2017).

[21] A. N. Gowda, M. Kumar, A. R. Thomas, R. Philip, and S. Kumar, Self-assembly of silver and gold nanoparticles in a metal-free phthalocyanine liquid crystalline matrix: structural, thermal, electrical and nonlinear optical characterization, Chem. Sel. **1**, 1361 (2016).

[22] T. Vimal, S. K. Gupta, R. Katiyar, A. Srivastava, M. Czerwinski, K. Krup, S. Kumar, and R. Manohar, Effect of metallic silver nanoparticles on the alignment and relaxation behaviour of liquid crystalline material in smectic C* phase. J. Appl. Phys. **122**, 114102 (2017).

[23] G. H. Pujar, N. Deshapande, I. A. M. Khazi, and S. R. Inamdar, Solvatochromism of a highly conjugated novel donor-π-acceptor dipolar fluorescent probe and its application in surface-energy transfer with gold nanoparticles, J. Mol. Liq. **271**, 118 (2018).

[24] Y. Ren, Q. Xin, X.-T. Tao, L. Wang, X.-Q. Yu, J.-X. Yang, and M.-H. Jiang, Novel multi-branched organic compounds with enhanced two-photon absorption benefiting from the strong electronic coupling, Chem. Phys. Lett. **414**, 253 (2005).

[25] T. S. Moss, Theory of intensity dependence of refractive index, Phys. Status Solidi (b) **101**, 555 (1980).

[26] A. L. González, C. Noguez, G. P. Ortiz, and G. Rodríguez-Gattorno, Optical absorbance of colloidal suspensions of silver polyhedral nanoparticles, J. Phys. Chem. B **109**, 17512 (2005).

[27] A. Slistan-Grijalva, R. Herrera-Urbina, J. F. Rivas-Silva, M. Ávalos-Borja, F. F. Castillón-Barrazad, and A. Posada-Amarillase, Classical theoretical characterization of the surface plasmon absorption band for silver spherical nanoparticles suspended in water and ethylene glycol, Physica E **27**, 104 (2004).

[28] S. Khatua, P. Manna, W.-S. Chang, A. Tcherniak, E. Friedlander, E. R. Zubarev, and S. Link, Plasmonic nanoparticles−liquid crystal composites, J. Phys. Chem. C **114**, 7251 (2010).

[29] G. Si, Y. Zhao, E. S. P. Leong, and Y. J. Liu, Liquid-crystal-enabled active plasmonics: a review, Materials **7**, 1296 (2014).

[30] A. Moroz, Localized resonances of composite particles, J. Phys. Chem. C **113**, 21604 (2009).

[31] T. Förster, Intermolecular energy migration and fluorescence, Ann. Phys. **437**, 55 (1948).

[32] J. R. Lakowicz, *Principles of Fluorescence Spectroscopy*, 2nd ed. (Kluwer Academic/Plenum, New York, 1999).

[33] C. S. Yun, A. Javier, T. Jennings, M. Fisher, S. Hira, S. Peterson, B. Hopkins, N. O. Reich, and G. F. J. Strouse, Nanometal surface energy transfer in optical rulers, breaking the FRET barrier, Am. Chem. Soc. **127**, 3115 (2005).

[34] J. Hohlbein, T. D. Craggs, and T. Cordes, Alternating-laser excitation: single-molecule FRET and beyond, Chem. Soc. Rev. **43**, 1156 (2014).

[35] T. L. Jennings, M. P. Singh, and G. F. Strouse, Fluorescent lifetime quenching near d = 1.5 nm gold nanoparticles: Probing NSET validity, J. Am. Chem. Soc. **128**, 5462 (2006).

[36] R. R. Chance, A. Prock, and R. Silbey, Molecular fluorescence and energy transfer near interfaces, Adv. Chem. Phys. **37**, 1 (1978).

[37] B. N. J. Persson and N. D. Lang, Electron-hole-pair quenching of excited states near a metal, Phys. Rev. B **26**, 5409 (1982).

[38] D. V. ÓConnor and D. Phillips, *Time-Correlated Single-Photon Counting* (Academic, New York, 1984).

[39] G. H. Pujar, N. Deshapande, M. S. Sannaikar, M. N. Wari, I. A. M. Khazi, and S. R. Inamdar, Synthesis, photophysics of a novel green light emitting 1,3,4-oxadiazole and its application in FRET with ZnSe/ZnS QDs donor, J. Mol. Liq. **248**, 350 (2017).

[40] A. Paul and A. Samanta, Photoinduced electron transfer reaction in room temperature ionic liquids: A combined laser flash photolysis and fluorescence study, J. Phys. Chem. B **111**, 1957 (2007).